

Model-independent Higgs coupling measurements at the LHC using the $H \rightarrow ZZ \rightarrow 4\ell$ lineshape

Heather E. Logan^{1,*} and Jeff Z. Salvail^{2,†}

¹*Carleton University, Ottawa, Ontario K1S 5B6, Canada*

²*University of Ottawa, Ottawa, Ontario K1N 6N5, Canada*

(Dated: July 21, 2011)

We show that combining a direct measurement of the Higgs total width from the $H \rightarrow ZZ \rightarrow 4\ell$ lineshape with Higgs signal rate measurements allows Higgs couplings to be extracted in a model-independent way from CERN Large Hadron Collider (LHC) data. Using existing experimental studies with 30 fb^{-1} at one detector of the 14 TeV LHC, we show that the couplings-squared of a 190 GeV Higgs to WW , ZZ , and gg can be extracted with statistical precisions of about 10%, and a 95% confidence level upper limit on an unobserved component of the Higgs decay width of about 22% of the SM Higgs width can be set. The method can also be applied for heavier Higgs masses.

arXiv:1107.4342v1 [hep-ph] 21 Jul 2011

* logan@physics.carleton.ca

† jsalv039@uottawa.ca

I. INTRODUCTION

The Higgs mechanism for electroweak symmetry breaking and generation of fermion masses remains the last untested component of the Standard Model (SM). The discovery of the physical Higgs boson that accompanies this mechanism, or its refutation through the discovery of alternative dynamics underlying electroweak symmetry breaking, is the primary goal of the CERN Large Hadron Collider (LHC). The SM Higgs mechanism predicts the couplings of the Higgs boson to pairs of SM particles in terms of the known particle masses. In extensions of the SM Higgs sector, these couplings are typically modified, with the pattern of modifications providing valuable information that can shed light on the structure of the extended model. A key test of the SM Higgs mechanism thus involves measurement of as many Higgs couplings as possible.

High-precision, model-independent measurements of Higgs couplings are a major component of the physics case for the International Linear e^+e^- Collider (ILC) [1]. Key to the model-independence of these measurements is the ability to measure the total production cross section for $e^+e^- \rightarrow ZH$ using the recoil-mass technique [2]. This technique requires event-by-event knowledge of the four-momentum of the initial state (without using measurements of the Higgs decay products), and is thus unavailable at the LHC. Instead, extraction of Higgs couplings from future LHC measurements of Higgs production and decay rates requires making a model-dependent assumption, either about the possible Higgs decay modes or about some of the Higgs couplings.

The difficulty arises due to a genuine flat direction in the coupling fit corresponding to allowing an unobserved Higgs decay mode while simultaneously increasing all the production and decay couplings by a common factor. The Higgs signal rate in production channel i and decay channel j is given by

$$\text{Rate}_{ij} = \sigma_i \text{BR}_j = \sigma_i \frac{\Gamma_j}{\Gamma_{\text{tot}}}, \quad (1)$$

where σ_i is the cross section for production channel i , BR_j is the Higgs branching ratio into final state j , Γ_j is the Higgs partial width into final state j , and Γ_{tot} is the Higgs total width. Adding a new, unobserved Higgs decay channel with partial width Γ_{new} while simultaneously increasing all the Higgs couplings by a common factor a relative to their SM values yields

$$\text{Rate}_{ij} = a^2 \sigma_i^{\text{SM}} \frac{a^2 \Gamma_j^{\text{SM}}}{a^2 \Gamma_{\text{tot}}^{\text{SM}} + \Gamma_{\text{new}}}. \quad (2)$$

For any given value of Γ_{new} , an appropriate choice of a yields Higgs signal rates identical to those in the SM.

Previous studies of Higgs coupling extraction from LHC data have dealt with this flat direction either by assuming that no unexpected Higgs decay channels exist [3–5], or by assuming that the Higgs couplings to WW and ZZ are bounded from above by their SM value [6].¹ These analyses have focused on Higgs masses between 100 and 190 GeV where many different Higgs production and decay modes are experimentally accessible. Depending on the Higgs mass, they have shown that LHC measurements will provide sensitivity to the Higgs couplings to W and Z pairs, top and bottom quarks, and tau leptons, as well as to potential new loop contributions to the Higgs couplings to photon and gluon pairs. Theoretical and systematic uncertainties play an important role in the fits [5, 6], and in general the extracted coupling values are correlated with one another [5].

In this paper we propose a method by which the model dependence can be removed from Higgs coupling measurements at the LHC. When the total width of the Higgs is above about a GeV, it can be measured directly using the lineshape of the four-lepton invariant mass distribution in $H \rightarrow ZZ \rightarrow 4\ell$, where $\ell = e, \mu$. This occurs in the SM for Higgs masses above about 190 GeV.² Such a measurement directly determines the denominator in Eqs. (1) and (2), removing the degeneracy in the fit without imposing any model assumptions.

The rest of this paper is organized as follows. In Sec. II we describe our parameterization of possible new physics in the Higgs couplings. In Sec. III we list the Higgs observables that we use in the fit and describe the fitting procedure. For a Higgs mass of 190 GeV, current LHC studies indicate that the only observable SM Higgs production modes will be gluon fusion and vector boson fusion and the only observable SM decays will be to WW and ZZ . Our fit is thus sensitive only to the Higgs couplings to WW and ZZ , to the effective Higgs coupling to two gluons, and to a possible new component of the Higgs total width. In Sec. IV we present the results of our fits as chi-squared contours in two-dimensional projections of our parameter space, as well as giving 1- and 2-sigma constraints on the couplings, assuming the best-fit point is at their SM values. In Sec. V we discuss our results and conclude.

¹ The latter assumption holds in any extended Higgs sector that contains only regular $SU(2)_L$ doublets and singlets. Viable models in which it is violated include the Georgi-Machacek model with $SU(2)_L$ -triplet Higgses [7, 8] and the Lee-Wick Standard Model [9] which solves the hierarchy problem by implementing Pauli-Villars regularization with physical fields [10]. The potential enhancements of the Higgs couplings to WW and ZZ above their SM values in these models have been studied in Refs. [11] and [12], respectively.

² The global fit to precision electroweak observables in the SM puts an upper bound on the SM Higgs mass of 169 (200) GeV at 95% (99%) confidence level [13]. Thus, Higgs masses heavy enough to resolve the Higgs total width from the $H \rightarrow ZZ \rightarrow 4\ell$ lineshape are disfavored in the context of the SM. However, in extended models, Higgs masses above 190 GeV are fully consistent with electroweak precision measurements; see Ref. [13] for an extensive review. Therefore, if such a heavy Higgs boson is discovered, the electroweak fit provides strong motivation to search for new physics effects, including shifts in the Higgs couplings relative to the SM expectations.

II. PARAMETERIZATION OF HIGGS COUPLINGS

A SM Higgs boson with mass 190 GeV decays 78.70% of the time to W^+W^- and 20.77% to ZZ , with the remaining 0.53% of decays mainly to $b\bar{b}$ and gg , leading to a total width of 1.036 GeV (computed using the public FORTRAN code `HDECAY` [14]). The largest production cross sections for such a Higgs boson at the LHC are gluon fusion ($gg \rightarrow H$) and vector boson fusion ($VBF \rightarrow H$). At this mass, LHC measurements will provide access to the Higgs total width through the $H \rightarrow ZZ \rightarrow 4\ell$ lineshape, as well as event rates in four primary Higgs production and decay channels: $gg \rightarrow H \rightarrow WW$, $gg \rightarrow H \rightarrow ZZ$, $VBF \rightarrow H \rightarrow WW$, and $VBF \rightarrow H \rightarrow ZZ$. LHC measurements can thus provide sensitivity to the Higgs couplings to WW and ZZ (through Higgs decays to these final states and through production via vector boson fusion), the effective coupling to gg (through production via gluon fusion), and potential new contributions to the Higgs total width (directly through the $H \rightarrow ZZ \rightarrow 4\ell$ lineshape as well as indirectly through the Higgs branching ratios to WW and ZZ final states).

We parameterize shifts in these three couplings in terms of three multiplicative factors, \bar{g}_W , \bar{g}_Z , and \bar{g}_g , which are all equal to 1 in the SM. We parameterize shifts in the Higgs total width in terms of a new, unobserved contribution to the width, Γ_{new} , which is zero in the SM. In terms of these parameters, the Higgs partial and total widths and production cross sections are given as follows (we neglect SM contributions to Γ_{tot} other than WW and ZZ):

$$\begin{aligned}\Gamma_W &= \bar{g}_W^2 \Gamma_W^{\text{SM}}, \\ \Gamma_Z &= \bar{g}_Z^2 \Gamma_Z^{\text{SM}}, \\ \Gamma_{\text{tot}} &= \Gamma_W + \Gamma_Z + \Gamma_{\text{new}}, \\ \sigma(gg \rightarrow H) &= \bar{g}_g^2 \sigma^{\text{SM}}(gg \rightarrow H), \\ \sigma(VBF \rightarrow H) &\simeq \bar{g}_W^2 \sigma_W^{\text{SM}} + \bar{g}_Z^2 \sigma_Z^{\text{SM}} \simeq [0.73 \bar{g}_W^2 + (1 - 0.73) \bar{g}_Z^2] \sigma^{\text{SM}}(VBF \rightarrow H).\end{aligned}\tag{3}$$

Two comments are in order. First, vector boson fusion proceeds through diagrams involving either W or Z exchange in the t -channel. If we take $\bar{g}_W = \bar{g}_Z \equiv \bar{g}_V$ as predicted in most extended Higgs models, then the cross section for vector boson fusion is given simply by $\sigma(VBF \rightarrow H) = \bar{g}_V^2 \sigma^{\text{SM}}(VBF \rightarrow H)$. If, however, we want to fit separately for \bar{g}_W^2 and \bar{g}_Z^2 (which are unequal, for example, in the Georgi-Machacek model [7, 8] with custodial $SU(2)$ violation in the Higgs mixing [11]), we must express the vector boson fusion cross section in terms of the separate contributions of the W and Z exchange diagrams. These diagrams do interfere, e.g., in $ud \rightarrow udH$; however, the interference is negligible as can be understood by examining the kinematics of the W and Z exchange diagrams: in W exchange the final-state u quark is produced primarily in the same direction as the initial d quark, while in Z exchange it is produced primarily in the opposite direction. We have checked this numerically using the public code `MadGraph` [15] by computing the tree-level cross section for $pp \rightarrow jjH$ and comparing it to the sum of the cross section including only W exchange and the cross section including only Z exchange. From this calculation we obtain the factors of 0.73 and $(1 - 0.73)$ for the W and Z fractions of the vector boson fusion cross section quoted in the last line of Eq. (3).

Second, the LHC measurements that we consider do not provide access to Higgs couplings to fermions. The cross section for $gg \rightarrow H$ is sensitive to the Higgs coupling to the top quark, which dominates the one-loop gluon fusion process in the SM; however, new colored particles running in the loop can also affect $gg \rightarrow H$ and their effects cannot be disentangled from a shift in the Higgs coupling to the top quark based on this single measurement. A large enhancement of the Higgs coupling to bottom quarks can lead to a non-negligible branching fraction for $H \rightarrow b\bar{b}$; we capture this possibility here only in Γ_{new} . A large enhancement of the Higgs coupling to bottom quarks can also affect the $gg \rightarrow H$ cross section through the contribution of the bottom quark in the loop. In this case, tree-level Higgs production through $b\bar{b} \rightarrow H$ can also become a significant contributor to the inclusive Higgs production cross section, so that the value of \bar{g}_g^2 extracted through our fit will be contaminated with this additional production mode. Searching for $gb \rightarrow Hb$ production with an extra tagged b quark in the final state could help pin down this scenario. We do not pursue this possibility further here.

Starting from the SM prediction for the event rate in each channel and the Higgs total width, the parameterization in Eq. (3) lets us recompute these rates and total width for any point in the four-dimensional parameter space of \bar{g}_W^2 , \bar{g}_Z^2 , \bar{g}_g^2 , and Γ_{new} . By comparing these model predictions to the expected experimental precision on the observables, we will determine the precision with which the four parameters can be measured.

III. OBSERVABLES AND FITTING PROCEDURE

We now describe the observables used in our fit and the fitting procedure. Our fit involves seven observables, comprising the Higgs total width and event rates in six production and decay channels. Our observables are each normalized to the corresponding SM expectation, so that in the SM their values are equal to 1. We take the expected

Observable	Process	N_S	N_B	Uncertainty	R_{gg}	R_{VBF}
\mathcal{O}_2	$H \rightarrow ZZ \rightarrow 4\ell$	68.1 (gg) + 11.2 (VBF)	50.4	14.4%	85.9%	14.1%
\mathcal{O}_3	$H \rightarrow ZZ \rightarrow 4\ell$	15.2 (VBF) + 3.14 (gg)	0.72	23.8%	17.1%	82.9%
\mathcal{O}_4	$H \rightarrow WW \rightarrow \ell\ell$	269 (gg) + 7.63 (VBF)	428	9.60%	97.2%	2.8%
\mathcal{O}_5	$H \rightarrow WW \rightarrow e\mu$	78.0 (VBF) + 6.60 (gg)	51.9	13.8%	7.8%	92.2%
\mathcal{O}_6	$H \rightarrow WW \rightarrow ee, \mu\mu$	73.2 (VBF) + 5.70 (gg)	55.8	14.7%	7.2%	92.8%

TABLE I. Higgs signal and background rates for observables \mathcal{O}_2 through \mathcal{O}_6 , from Ref. [17]. Here ℓ includes e and μ . Event numbers are for 30 fb^{-1} . The statistical uncertainty on the signal rate is given by $\sqrt{N_S + N_B}/N_S$. We also quote the fractions of the signal events coming from gluon fusion (R_{gg}) and vector boson fusion (R_{VBF}) for each rate observable.

experimental uncertainties on these observables from the literature. These expected uncertainties have been evaluated for 30 fb^{-1} of integrated luminosity at one detector at the 14 TeV center-of-mass energy LHC, and include statistical uncertainties only. We do not attempt to incorporate systematic uncertainties in the fit.

Our first observable is the Higgs total width,

$$\mathcal{O}_1 = \frac{\Gamma_{\text{tot}}}{\Gamma_{\text{tot}}^{\text{SM}}} = \frac{\bar{g}_W^2 \Gamma_W^{\text{SM}} + \bar{g}_Z^2 \Gamma_Z^{\text{SM}} + \Gamma_{\text{new}}}{\Gamma_W^{\text{SM}} + \Gamma_Z^{\text{SM}}}. \quad (4)$$

Extraction of the Higgs total width from the $H \rightarrow ZZ \rightarrow 4\ell$ lineshape has been studied most thoroughly by CMS [16]. For an integrated luminosity of 30 fb^{-1} , CMS finds a statistical uncertainty on Γ_{tot} of 17.6% for $M_H = 190 \text{ GeV}$ (see Sec. 10.2.1.7 of Ref. [16]). Because this uncertainty comes solely from the statistical precision in measuring the Gaussian width of the Higgs lineshape, it scales in the usual way as $(\int \mathcal{L})^{-1/2}$, where $\int \mathcal{L}$ is the integrated luminosity. The uncertainty in the intrinsic 4ℓ invariant mass resolution will enter as a systematic uncertainty, but has not been included in the analysis of Ref. [16].

Our next five observables are Higgs signal event rates studied for ATLAS in Ref. [17]. These comprise signal rates for Higgs production via gluon fusion and vector boson fusion, with decays to WW and ZZ final states (the vector boson fusion channel with decays to WW is divided into two channels, one with $e\mu$ in the final state and the other with ee or $\mu\mu$). Because the signal and background selections in Ref. [17] were done specifically for the purpose of Higgs coupling extraction, the author took care to account for the “contamination” of the signal in one production mode by Higgs production via the other production mode: for example, the event selections for Higgs production via gluon fusion contain some events in which the Higgs is produced by vector boson fusion, and vice versa. Signal and background event numbers from Ref. [17] are summarized in Table I. Observables \mathcal{O}_2 and \mathcal{O}_4 select predominantly for Higgs production via gluon fusion, while \mathcal{O}_3 , \mathcal{O}_5 , and \mathcal{O}_6 select predominantly for Higgs production via vector boson fusion. For our fit, we define these observables as the rate for the selected process normalized to the SM rate:

$$\mathcal{O}_i = \frac{\text{Rate}_i}{\text{Rate}_i^{\text{SM}}} = R_{gg}^i \frac{\sigma(gg \rightarrow H) \text{BR}_i}{\sigma^{\text{SM}}(gg \rightarrow H) \text{BR}_i^{\text{SM}}} + R_{\text{VBF}}^i \frac{\sigma(\text{VBF} \rightarrow H) \text{BR}_i}{\sigma^{\text{SM}}(\text{VBF} \rightarrow H) \text{BR}_i^{\text{SM}}}, \quad i = 2 \dots 6, \quad (5)$$

where R_{gg}^i and R_{VBF}^i are the fractions of signal events coming from gluon fusion and vector boson fusion, respectively, as given in Table I. Using Eq. (3), these observables can be expressed in terms of our fit parameters as

$$\begin{aligned} \mathcal{O}_i &= \{R_{gg}^i \bar{g}_g^2 + R_{\text{VBF}}^i [0.73 \bar{g}_W^2 + (1 - 0.73) \bar{g}_Z^2]\} \bar{g}_Z^2 \frac{\Gamma_{\text{tot}}^{\text{SM}}}{\Gamma_{\text{tot}}}, \quad i = 2, 3, \\ \mathcal{O}_i &= \{R_{gg}^i \bar{g}_g^2 + R_{\text{VBF}}^i [0.73 \bar{g}_W^2 + (1 - 0.73) \bar{g}_Z^2]\} \bar{g}_W^2 \frac{\Gamma_{\text{tot}}^{\text{SM}}}{\Gamma_{\text{tot}}}, \quad i = 4, 5, 6, \end{aligned} \quad (6)$$

where the ratio $\Gamma_{\text{tot}}/\Gamma_{\text{tot}}^{\text{SM}}$ has been given in terms of the fit parameters in Eq. (4).

Our last observable comes from a CMS analysis of Higgs production in vector boson fusion with decays to WW in the channel $jj\ell\nu$ [18]. The analysis in Ref. [18] did not take into account any “contamination” of the signal by Higgs production via gluon fusion; we take this at face value for the purpose of our fit. The observable is the ratio of the signal rate to its SM value, which can be expressed as

$$\mathcal{O}_7 = [0.73 \bar{g}_W^2 + (1 - 0.73) \bar{g}_Z^2] \bar{g}_W^2 \frac{\Gamma_{\text{tot}}^{\text{SM}}}{\Gamma_{\text{tot}}}, \quad (7)$$

where again the ratio $\Gamma_{\text{tot}}/\Gamma_{\text{tot}}^{\text{SM}}$ has been given in terms of the fit parameters in Eq. (4). After cuts, Ref. [18] found a signal cross section of 2.340 fb and a background cross section of 1.567 fb , leading to a statistical uncertainty of 15.4% in 30 fb^{-1} .

We note that the statistical power of the $H \rightarrow ZZ$ channels could be improved by including $\ell\ell\nu\nu$ and $\ell\ell b\bar{b}$ final states. These have been studied as LHC Higgs discovery channels; ATLAS [19] has studied both channels for $M_H \geq 200$ GeV, while CMS [20] has studied $\ell\ell\nu\nu$ for $M_H \geq 200$ GeV and $\ell\ell b\bar{b}$ for $M_H \geq 300$ GeV.

In order to evaluate the precision with which these LHC measurements would be able to constrain the Higgs couplings, we compute a χ^2 for each choice of the parameters $(\bar{g}_W^2, \bar{g}_Z^2, \bar{g}_g^2, \Gamma_{\text{new}})$ according to

$$\chi^2 = \sum_{i=1}^7 \frac{(\mathcal{O}_i - \mathcal{O}_i^{\text{SM}})^2}{\sigma_i^2}, \quad (8)$$

where our observables are normalized such that $\mathcal{O}_i^{\text{SM}} = 1$ and σ_i is the (fractional) uncertainty on observable \mathcal{O}_i . This amounts to assuming that the measured values of all the observables are equal to the SM prediction; thus $\chi^2 = 0$ at the SM point $(\bar{g}_W^2, \bar{g}_Z^2, \bar{g}_g^2, \Gamma_{\text{new}}) = (1, 1, 1, 0)$. Note that we ignore correlated uncertainties, the most important of which we expect to be the luminosity uncertainty (which affects \mathcal{O}_2 through \mathcal{O}_7), the theoretical uncertainty on the gluon fusion cross section (which affects \mathcal{O}_2 through \mathcal{O}_6), and the theoretical uncertainty on the weak boson fusion cross section (which affects \mathcal{O}_2 through \mathcal{O}_7). Uncertainty on the background normalization for the channels with $H \rightarrow WW$ may also be important, and affects \mathcal{O}_4 through \mathcal{O}_7 .

We perform two sets of fits: one with three free parameters $(\bar{g}_V^2, \bar{g}_g^2, \Gamma_{\text{new}}/\Gamma_{\text{tot}}^{\text{SM}})$, in which we take $\bar{g}_W^2 = \bar{g}_Z^2 \equiv \bar{g}_V^2$; and one with four free parameters $(\bar{g}_W^2, R, \bar{g}_g^2, \Gamma_{\text{new}}/\Gamma_{\text{tot}}^{\text{SM}})$, where

$$R \equiv \frac{\bar{g}_Z^2}{\bar{g}_W^2}. \quad (9)$$

We choose R as the fourth variable instead of \bar{g}_Z^2 because we are most interested in how well the LHC will be able to test the prediction $\bar{g}_W = \bar{g}_Z$ of extended Higgs models that contain only Higgs doublets and singlets. When presenting our results we normalize the new contribution to the Higgs total width to the SM Higgs total width, thus plotting limits on the dimensionless quantity $\Gamma_{\text{new}}/\Gamma_{\text{tot}}^{\text{SM}}$.

In each case we scan over the free parameters and compute χ^2 at each parameter point. We then project the χ^2 distribution down onto two or one parameters by marginalizing over the undisplayed parameters—in other words, we find the smallest value of χ^2 that can be obtained by varying the undisplayed parameters. In each case we plot the resulting 1σ , 2σ , and 3σ constraints. Projecting onto one parameter, this corresponds to $\chi^2 = 1, 4$, and 9 . Projecting onto two parameters, this corresponds to $\chi^2 = 2.296, 6.180$, and 11.829 .

We will also display results extrapolated to an integrated luminosity of 100 fb^{-1} . Because all our uncertainties are statistical, we can do this simply by scaling all uncertainties by $(\int \mathcal{L})^{-1/2}$, i.e., by multiplying the uncertainties for 30 fb^{-1} by $\sqrt{3/10}$. All results presented assume data from only one detector—combining data from ATLAS and CMS would effectively double the statistics.

IV. RESULTS

We begin by scanning over the three-dimensional parameter space of $(\bar{g}_V^2, \bar{g}_g^2, \Gamma_{\text{new}}/\Gamma_{\text{tot}}^{\text{SM}})$, with $\bar{g}_V^2 \equiv \bar{g}_W^2 = \bar{g}_Z^2$, using the uncertainties corresponding to 30 fb^{-1} of integrated luminosity to calculate the χ^2 . Results are shown in Fig. 1, in which we plot the projections of the χ^2 distribution onto the three pairs of variables as well as onto each individual variable. The solid contours correspond to the 1σ , 2σ , and 3σ constraints. The straight dashed lines show the 1σ , 2σ , and 3σ ranges of the individual parameters. Because we compute the χ^2 assuming that the “observed” values of the inputs are equal to their SM predictions, the minimum value of the χ^2 is zero and occurs at $(\bar{g}_V^2, \bar{g}_g^2, \Gamma_{\text{new}}/\Gamma_{\text{tot}}^{\text{SM}}) = (1, 1, 0)$. We see that \bar{g}_V^2 and \bar{g}_g^2 can be measured with about 8.5% and 11% precision respectively, and $\Gamma_{\text{new}}/\Gamma_{\text{tot}}^{\text{SM}}$ is bounded to be below about 22% at the 2σ level. 1σ , 2σ , and 3σ ranges for each of the parameters are summarized in Table II.

Scaling the statistical uncertainties to an integrated luminosity of 100 fb^{-1} tightens the constraints as shown in Fig. 2. This reduces the uncertainties on \bar{g}_V^2 and \bar{g}_g^2 to about 4.6% and 5.8% respectively, and lowers the 2σ upper limit on $\Gamma_{\text{new}}/\Gamma_{\text{tot}}^{\text{SM}}$ to about 12%. We emphasize here that at this level of statistical precision, we expect that systematic uncertainties, which have not been included in our fit, will begin to play a significant role.

Notice in both Figs. 1 and 2 that $\Gamma_{\text{new}}/\Gamma_{\text{tot}}^{\text{SM}}$ is positively correlated with both \bar{g}_g^2 and \bar{g}_V^2 . This is a manifestation of the flat direction discussed in the introduction, which has been lifted by the inclusion of the direct measurement of the Higgs total width in the fit. To illustrate the importance of the total width measurement, we redo the fit for 30 fb^{-1} with the uncertainty on the total width measurement artificially inflated from 17.6% to 100%. Results are shown in Fig. 3.

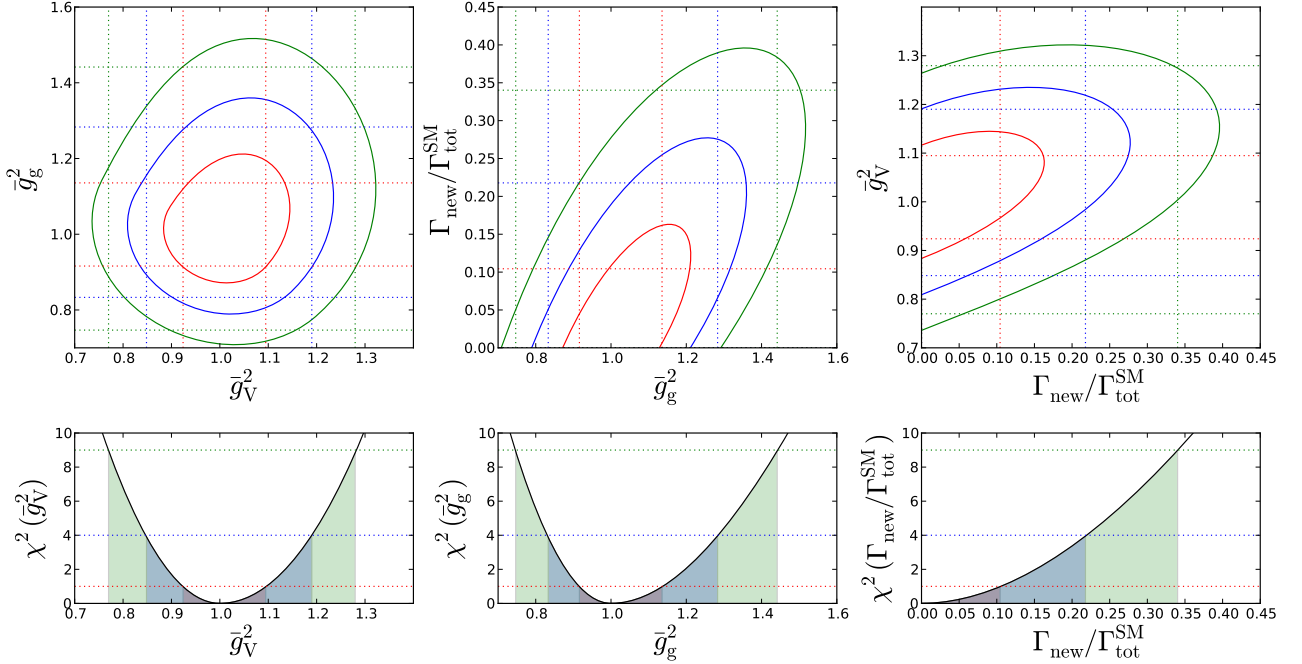


FIG. 1. Results of the three-parameter scan over $(\bar{g}_V^2, \bar{g}_g^2, \Gamma_{\text{new}}/\Gamma_{\text{tot}}^{\text{SM}})$, with $\bar{g}_W^2 = \bar{g}_Z^2 \equiv \bar{g}_V^2$, for $M_H = 190$ GeV and 30 fb^{-1} of integrated luminosity. The upper plots show the 1σ , 2σ , and 3σ regions for each pair of parameters with the χ^2 marginalized over the remaining parameter. The lower plots show the marginalized χ^2 distributions for each parameter, with the shaded regions indicating the 1σ , 2σ , and 3σ ranges. These ranges for each parameter are indicated on the upper plots by the straight dotted lines.

Parameter	$\int \mathcal{L}$	1σ	2σ	3σ
\bar{g}_V^2	30 fb^{-1}	0.924–1.095	0.848–1.190	0.770–1.280
	100 fb^{-1}	0.960–1.053	0.918–1.103	0.876–1.154
\bar{g}_g^2	30 fb^{-1}	0.916–1.136	0.833–1.283	0.747–1.442
	100 fb^{-1}	0.956–1.071	0.909–1.150	0.862–1.229
$\Gamma_{\text{new}}/\Gamma_{\text{tot}}^{\text{SM}}$	30 fb^{-1}	0–0.104	0–0.218	0–0.340
	100 fb^{-1}	0–0.056	0–0.115	0–0.176

TABLE II. Parameter ranges allowed at 1σ , 2σ , and 3σ by the three-parameter fit, with 30 fb^{-1} or 100 fb^{-1} of integrated luminosity. Here $\bar{g}_W^2 = \bar{g}_Z^2 \equiv \bar{g}_V^2$.

Finally, we scan over the four-dimensional parameter space of $(\bar{g}_W^2, R, \bar{g}_g^2, \Gamma_{\text{new}}/\Gamma_{\text{tot}}^{\text{SM}})$, with $R \equiv \bar{g}_Z^2/\bar{g}_W^2$. The resulting constraints on \bar{g}_W^2 and R are shown for 30 fb^{-1} and 100 fb^{-1} in the left and right panels of Fig. 4. We see that R can be measured with a precision of about 14% with 30 fb^{-1} , improving to about 8% with 100 fb^{-1} (again we emphasize that these uncertainties are statistical only). The precisions on the other three parameters are comparable to those in the three-parameter fit. 1σ , 2σ , and 3σ ranges for each of the parameters are summarized in Table III. Note that due to the finite spacing of our four-parameter scan grids, the quoted uncertainties are only accurate to within about 2 percentage points.

For comparison, we can estimate the precision with which R can be measured by taking the ratio of Higgs signal rates with a common production mode but with decays to ZZ versus WW . In such a ratio the production cross section and Higgs total width cancel, leaving the ratio of the partial widths of $H \rightarrow ZZ$ and $H \rightarrow WW$, each of which is proportional to the square of the respective coupling. In particular, for Higgs production via gluon fusion we can take the ratio of \mathcal{O}_2 and \mathcal{O}_4 , while for Higgs production via vector boson fusion we can take the ratio of \mathcal{O}_3 and a combination of \mathcal{O}_5 , \mathcal{O}_6 , and \mathcal{O}_7 . Propagating the uncertainties in the usual way, we find an uncertainty on R of

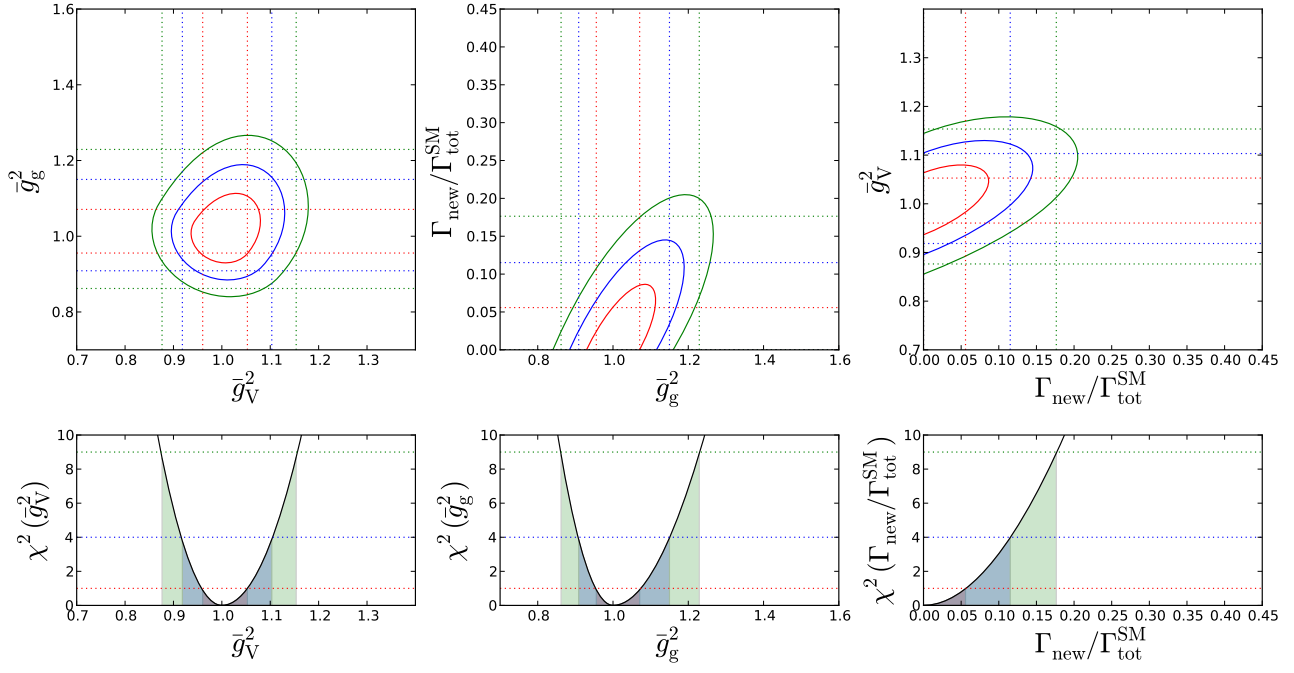


FIG. 2. As in Fig. 1 but for 100 fb⁻¹ of integrated luminosity.

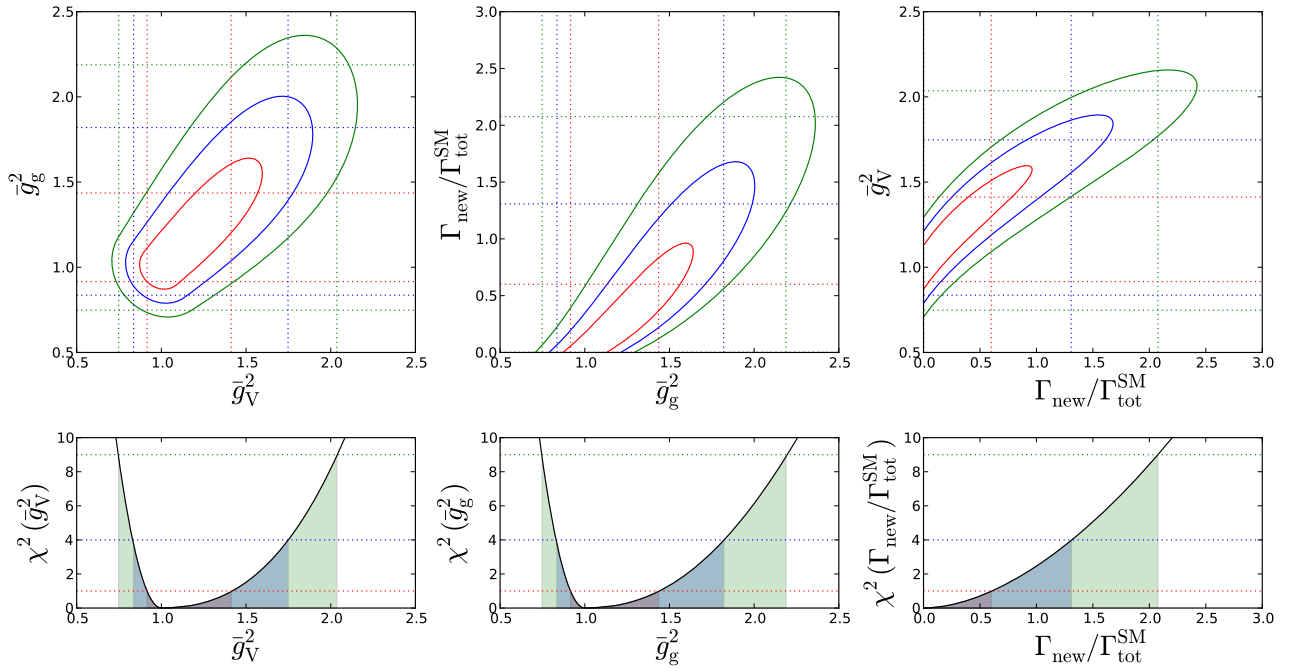


FIG. 3. As in Fig. 1 but with the uncertainty on the measurement of $\Gamma_{\text{tot}}/\Gamma_{\text{tot}}^{\text{SM}}$ artificially set to 100%. Note the expanded range of the axes compared to Fig. 1.

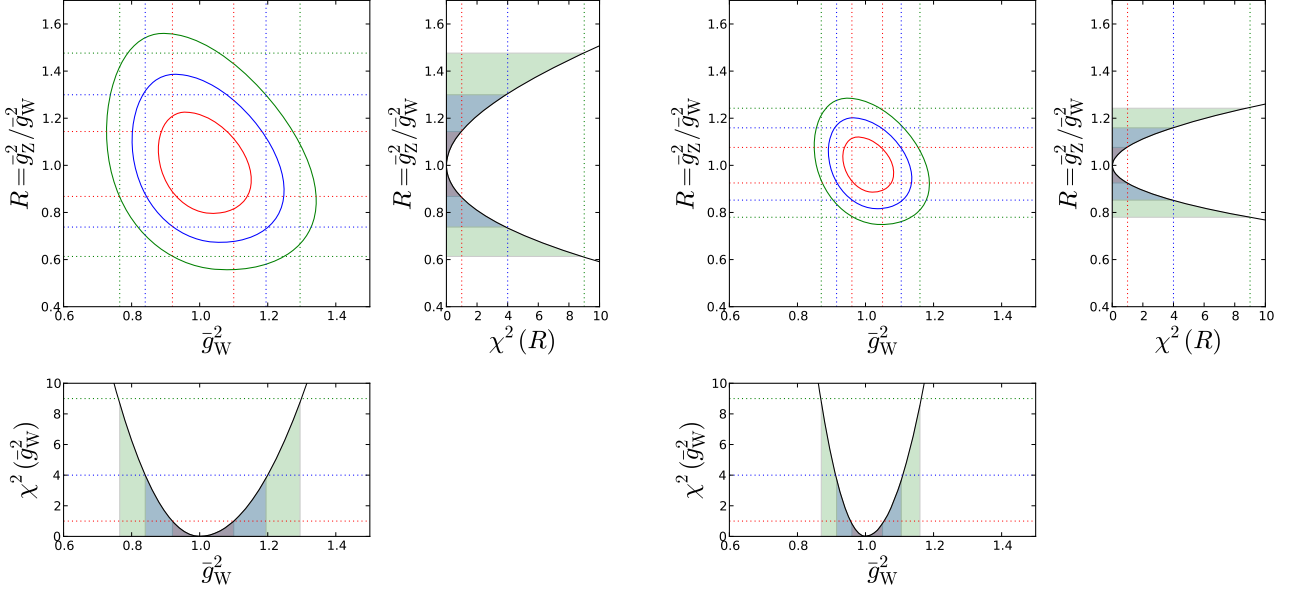


FIG. 4. Results of the four-parameter scan over $(\bar{g}_W^2, R, \bar{g}_g^2, \Gamma_{\text{new}}/\Gamma_{\text{tot}}^{\text{SM}})$, for $M_H = 190$ GeV and integrated luminosities of 30 fb^{-1} (left) and 100 fb^{-1} (right). We show the 1σ , 2σ , and 3σ regions for the pair of parameters (\bar{g}_W^2, R) with the χ^2 marginalized over the remaining two parameters. We also show the marginalized χ^2 distributions for each of these two parameters, with the shaded regions indicating the 1σ , 2σ , and 3σ ranges. These ranges for \bar{g}_W^2 and R are indicated on the two-dimensional plots by the straight dotted lines.

Parameter	$\int \mathcal{L}$	1σ	2σ	3σ
\bar{g}_W^2	30 fb^{-1}	0.92–1.10	0.84–1.20	0.77–1.30
	100 fb^{-1}	0.96–1.05	0.92–1.11	0.87–1.16
$R \equiv \bar{g}_Z^2/\bar{g}_W^2$	30 fb^{-1}	0.87–1.14	0.74–1.30	0.61–1.48
	100 fb^{-1}	0.93–1.08	0.85–1.16	0.78–1.24
\bar{g}_g^2	30 fb^{-1}	0.92–1.13	0.84–1.28	0.75–1.44
	100 fb^{-1}	0.96–1.07	0.91–1.15	0.86–1.23
$\Gamma_{\text{new}}/\Gamma_{\text{tot}}^{\text{SM}}$	30 fb^{-1}	0–0.10	0–0.21	0–0.34
	100 fb^{-1}	0–0.05	0–0.11	0–0.17

TABLE III. Parameter ranges allowed at 1σ , 2σ , and 3σ by the four-parameter fit, with 30 fb^{-1} or 100 fb^{-1} of integrated luminosity. Note that due to the finite spacing of our four-parameter scan grids, the quoted parameter range boundaries are only accurate to within about 0.02.

about 14% with 30 fb^{-1} and 7.8% with 100 fb^{-1} , very consistent with the results of the χ^2 scan. This ratio method is inexact due to the fact that the channels with different final states have different amounts of “contamination” of the desired production mode by the other production mode; i.e., R_{gg}^i and R_{VBF}^i are different for the \mathcal{O}_i in the numerator and the denominator, so that the parameter dependence in the production cross sections does not cancel perfectly.

V. DISCUSSION AND CONCLUSIONS

In this paper we showed that truly model-independent Higgs coupling measurements can be made at the LHC when the Higgs total width is experimentally accessible. For a SM-like Higgs, this occurs for $M_H \gtrsim 190$ GeV. At such high masses, however, the only accessible Higgs decay modes in the SM are to WW and ZZ , with production via gluon fusion or vector boson fusion. Thus the LHC measurements provide access to the Higgs couplings to WW and ZZ , the effective coupling to gluons, and any new contribution to the Higgs total width beyond the decay widths to WW

and ZZ .

Using existing LHC studies for a Higgs mass of 190 GeV at 14 TeV center-of-mass energy and considering only statistical uncertainties, we found that with 30 fb^{-1} at one detector the Higgs coupling-squared to vector bosons (assuming the ratio of WW and ZZ couplings is equal to its SM value) can be measured with an uncertainty of about 8.5%, the Higgs effective coupling-squared to gluons can be measured with an uncertainty of about 11%, and a new, non-SM component of the Higgs total width can be constrained at the 2σ level to be below about 22% of the SM Higgs total width at this mass. With 100 fb^{-1} at one detector the coupling-squared uncertainties decrease to about 4.6% and 5.8%, respectively, and the 2σ upper limit on a new contribution to the Higgs total width decreases to about 12% of the SM Higgs total width. At this level of precision we expect that systematic uncertainties will be important.

To give a sense of the usefulness of our constraint on a new contribution to the Higgs total width, consider Higgs decays to invisible final states such as dark matter particles. ATLAS has studied the sensitivity to invisible Higgs decays in vector boson fusion with 30 fb^{-1} at 14 TeV. For $M_H = 190 \text{ GeV}$ they find a 95% confidence level sensitivity to $\xi^2 \equiv [\sigma(\text{VBF} \rightarrow H)/\sigma^{\text{SM}}(\text{VBF} \rightarrow H)] \times \text{BR}(H \rightarrow \text{invis.})$ of about 15% not including systematic uncertainties, which rises to 60% including systematics [21]. Their dominant systematic uncertainty comes from the 10% background normalization uncertainty due to the theoretical uncertainty in the shape of the angular distribution of the two jets in the dominant Wjj and Zjj backgrounds; using a next-to-leading order calculation for Wjj and Zjj should reduce this by a factor of two, improving the 95% confidence level sensitivity to ξ^2 to roughly 40%. For SM-like Higgs couplings to WW and ZZ , this more optimistic limit corresponds to a new invisible component of the Higgs total width of $\Gamma_{\text{new}}/\Gamma_{\text{tot}}^{\text{SM}} \simeq 65\%$, which should be easily detectable (but not identifiable as an invisible decay) using our methods.

How do our results compare with those achievable at the ILC? Results of multiple ILC Higgs coupling studies at a variety of Higgs masses are summarized in Ref. [22], which incorporates results for e^+e^- center-of-mass energies of 350–800 GeV and integrated luminosities of 500–1000 fb^{-1} . While $M_H = 190 \text{ GeV}$ was not explicitly studied in Ref. [22], we can obtain coupling uncertainties for this mass from Fig. 5 of Ref. [22], which interpolates between higher and lower studied mass points. From this we read off an ILC uncertainty on \bar{g}_W^2 of about 3%, to be compared with our LHC statistical precision of 8.5% (4.6%) with 30 fb^{-1} (100 fb^{-1}). ILC has no access to \bar{g}_g^2 for this Higgs mass due to the extreme suppression of the $H \rightarrow gg$ branching fraction. The direct ILC measurement of the Higgs total width from the $H \rightarrow ZZ \rightarrow 4\ell$ lineshape is limited by statistics. However, it was shown in Ref. [23] that prospects seem good to measure the Higgs total width to better than 10% precision from the Higgs recoil mass lineshape in $e^+e^- \rightarrow ZH$, running at a center-of-mass energy not too far above the threshold for ZH associated production.

Of greater importance, however, are the complementary ILC measurements of the Higgs couplings to $b\bar{b}$ and $t\bar{t}$ that cannot be measured at the LHC for the relatively high Higgs mass considered here. Despite the very small branching fraction of $H \rightarrow b\bar{b}$ at $M_H = 190 \text{ GeV}$, \bar{g}_b^2 can be measured to about 14% precision at the ILC [22], where \bar{g}_b is a multiplicative factor parameterizing the shift in the $Hb\bar{b}$ coupling from its SM value. A detailed study of the measurement of the Higgs coupling to $t\bar{t}$ from the process $e^+e^- \rightarrow t\bar{t}H$, $H \rightarrow WW$ was made in Ref. [24], assuming 1000 fb^{-1} at an e^+e^- center-of-mass energy of 800 GeV. Interpolating the results of Ref. [24] to $M_H = 190 \text{ GeV}$, we can read off an uncertainty on \bar{g}_t^2 (defined analogously to \bar{g}_b^2) of about 21% (24%) for a residual background normalization uncertainty of 5% (10%). Combining this measurement of \bar{g}_t^2 with the LHC measurement of \bar{g}_g^2 allows one to probe contributions to the effective Hgg coupling due to particles other than the top quark.

We note that all the ILC coupling measurement precisions quoted here have been extracted with various model assumptions applied, rather than from a fully model-independent fit to ILC observables.

We now discuss systematic uncertainties. We expect the most important systematic uncertainties to be the luminosity uncertainty, theoretical and parton distribution function (PDF) uncertainties on the gluon fusion and vector boson fusion cross sections, the background normalization uncertainty particularly in the $H \rightarrow WW$ channels, and the uncertainty in the experimental resolution of the 4ℓ invariant mass used in the Higgs width determination. We comment on these as follows:

- Previous studies of Higgs coupling extraction from LHC data have assumed a luminosity uncertainty of 5% [3, 5, 6, 17]. Recent ATLAS [25] and CMS [26] luminosity determinations from data collected in 2010 have achieved uncertainties of 3.4% and 4.0%, respectively. Normalizing LHC rate measurements to the inclusive W or Z production rates, which are now known to next-to-next-to-leading order in QCD and with next-to-leading order electroweak corrections leading to a theoretical uncertainty below 1%, could replace the luminosity uncertainty with the small statistical and PDF uncertainties on the W or Z rate measurement.
- Recent improvements in the calculation of the gluon fusion Higgs production cross section have significantly reduced the theoretical uncertainty. The LHC Higgs Cross Section Working Group [27] quotes a conservative theoretical uncertainty of 8.4% and a PDF uncertainty of 6.8% for $M_H = 190 \text{ GeV}$ at the 14 TeV LHC (these numbers become 8.3% and 7.9% at 7 TeV center-of-mass energy). Other groups are more aggressive on the theory uncertainty; for example, Ref. [28] combines the most up-to-date calculations including renormalization-

group improvement of the QCD corrections at next-to-next-to-next-to-leading logarithmic accuracy as well as next-to-leading order electroweak corrections, and finds a remaining scale uncertainty of only 1.3% (1.5%) for 14 TeV (7 TeV) center-of-mass energy. The uncertainty on the gluon PDF is also expected to improve as LHC data become available to be incorporated into the global PDF fits.

- The cross section for Higgs production via vector boson fusion is now known through next-to-next-to-leading order in QCD and includes next-to-leading order electroweak corrections. The remaining theoretical scale uncertainty at the LHC is a mere 0.3% (0.2%) and the PDF uncertainty is 2.5% (2.6%) at 14 TeV (7 TeV) [27].
- For data-driven background determination, the background normalization uncertainty comes from the statistical uncertainty in the background control samples as well as the theoretical uncertainty in the extrapolation from the control regions into the signal region. In previous studies the most important of these has been the WW background, for which the number of events in the control region is no larger than in the signal region and the extrapolation error from shape uncertainty has been taken as 5% [6].
- The two-lepton invariant mass resolution should be well-calibrated from the Z peak. We expect that the four-lepton invariant mass resolution can be determined from this. We are not aware of a discussion of this uncertainty in the literature.

The Higgs lineshape and production rate measurement studies that we used in this analysis were all done for an LHC center-of-mass design energy of 14 TeV. The LHC is currently running at a center-of-mass energy of 7 TeV, however, and this lower-energy running is anticipated to continue to the end of 2012. The LHC experiments have already collected more than 1 fb^{-1} of data, and may be able to collect several fb^{-1} at this lower center-of-mass energy by the end of 2012. Because of this, it is interesting to consider how much data would be needed at 7 TeV to achieve the uncertainties obtained here for 14 TeV. For a mass of 190 GeV, Higgs signal cross sections in both gluon fusion and vector boson fusion are smaller by a factor of 3.8 [27] at 7 TeV compared to their values at 14 TeV. Combining data from both ATLAS and CMS, each experiment would need almost 60 fb^{-1} at 7 TeV to together collect the same number of signal events as used in our analysis of 30 fb^{-1} at one detector. A more quantitative estimate would require information on the background cross sections at 7 TeV, and possibly involve a new optimization of the signal selections.

ACKNOWLEDGMENTS

We thank Alain Bellerive for helpful discussions of statistics. H.E.L. was supported in part by the Natural Sciences and Engineering Research Council of Canada.

-
- [1] G. Aarons *et al.* [ILC Collaboration], arXiv:0709.1893 [hep-ph].
 - [2] P. Garcia-Abia and W. Lohmann, Eur. Phys. J. direct C **2**, 2 (2000) [arXiv:hep-ex/9908065].
 - [3] D. Zeppenfeld, R. Kinnunen, A. Nikitenko and E. Richter-Was, Phys. Rev. D **62**, 013009 (2000) [arXiv:hep-ph/0002036]; A. Djouadi *et al.*, arXiv:hep-ph/0002258.
 - [4] A. Belyaev and L. Reina, JHEP **0208**, 041 (2002) [arXiv:hep-ph/0205270].
 - [5] R. Lafaye, T. Plehn, M. Rauch, D. Zerwas and M. Dührssen, JHEP **0908**, 009 (2009) [arXiv:0904.3866 [hep-ph]].
 - [6] M. Dührssen, S. Heinemeyer, H. Logan, D. Rainwater, G. Weiglein and D. Zeppenfeld, Phys. Rev. D **70**, 113009 (2004) [arXiv:hep-ph/0406323].
 - [7] H. Georgi and M. Machacek, Nucl. Phys. B **262**, 463 (1985).
 - [8] M. S. Chanowitz and M. Golden, Phys. Lett. B **165**, 105 (1985); J. F. Gunion, R. Vega and J. Wudka, Phys. Rev. D **42**, 1673 (1990); Phys. Rev. D **43**, 2322 (1991).
 - [9] B. Grinstein, D. O'Connell and M. B. Wise, Phys. Rev. D **77**, 025012 (2008) [arXiv:0704.1845 [hep-ph]].
 - [10] T. D. Lee and G. C. Wick, Nucl. Phys. B **9**, 209 (1969); Phys. Rev. D **2**, 1033 (1970).
 - [11] H. E. Logan and M. A. Roy, Phys. Rev. D **82**, 115011 (2010) [arXiv:1008.4869 [hep-ph]].
 - [12] E. Alvarez, E. C. Leskow and J. Zurita, arXiv:1104.3496 [hep-ph].
 - [13] M. Baak *et al.*, arXiv:1107.0975 [hep-ph].
 - [14] A. Djouadi, J. Kalinowski and M. Spira, Comput. Phys. Commun. **108**, 56 (1998) [arXiv:hep-ph/9704448], code available from <http://people.web.psi.ch/spira/hdecay/>.
 - [15] J. Alwall *et al.*, JHEP **0709**, 028 (2007) [arXiv:0706.2334 [hep-ph]].
 - [16] G. L. Bayatian *et al.* [CMS Collaboration], J. Phys. G **34**, 995 (2007).
 - [17] M. Dührssen, ATL-PHYS-2003-030 (2003), available from <http://cdsweb.cern.ch>.

- [18] H. Pi, P. Avery, J. Rohlf, C. Tully, and S. Kunori, CMS-NOTE-2006-092 (2006), available from <http://cdsweb.cern.ch>.
- [19] ATLAS Collaboration, ATL-PHYS-PUB-2010-015 (2010), available from <http://cdsweb.cern.ch>.
- [20] CMS Collaboration, CMS-NOTE-2010-008 (2010), available from <http://cdsweb.cern.ch>.
- [21] G. Aad *et al.* [ATLAS Collaboration], arXiv:0901.0512 [hep-ex].
- [22] M. Battaglia, arXiv:hep-ph/0211461.
- [23] F. Richard and P. Bambade, arXiv:hep-ph/0703173.
- [24] A. Gay, Eur. Phys. J. C **49**, 489 (2007) [arXiv:hep-ph/0604034].
- [25] ATLAS Collaboration, ATLAS-CONF-2011-011 (2011), available from <http://cdsweb.cern.ch>.
- [26] CMS Collaboration, CMS-DP-2011-002 (2011), available from <http://cdsweb.cern.ch>.
- [27] S. Dittmaier *et al.* [LHC Higgs Cross Section Working Group], arXiv:1101.0593 [hep-ph].
- [28] V. Ahrens, T. Becher, M. Neubert and L. L. Yang, Phys. Lett. B **698**, 271 (2011) [arXiv:1008.3162 [hep-ph]].